ACS APPLIED MATERIALS & INTERFACES

Research Article

www.acsami.org

Thermal Annealing Induced Enhancements of Electrical Conductivities and Mechanism for Multiwalled Carbon Nanotubes Filled Poly(Ethylene-*co*-Hexene) Composites

Wenlin Li,[†] Yaqiong Zhang,[†] Jingjing Yang,[†] Jun Zhang,[‡] Yanhua Niu,*[,‡] and Zhigang Wang*[,†]

[†]CAS Key Laboratory of Soft Matter Chemistry, Department of Polymer Science and Engineering, Hefei National Laboratory for Physical Sciences at the Microscale, University of Science and Technology of China, Hefei, Anhui Province 230026, P. R. China

[‡]Institute of Chemistry, Chinese Academy of Sciences, Beijing, 100190, P. R. China

ABSTRACT: Thermal annealing-induced enhancements of electrical conductivities at the temperature higher than the melting point of poly(ethylene-*co*-hexene) matrix for multiwalled carbon nanotubes filled poly(ethylene-*co*-hexene) (MWCNTs/PEH) composites were investigated by electrical conductivity measurements. Two types of MWCNTs with low and high aspect ratios (4 and 31) were added as fillers into PEH matrix, respectively for comparison study purpose. The morphological changes due to annealing for MWCNTs/PEH composites were observed by SEM. The formation of MWCNT networks in the composites were clearly demonstrated by rheological measurements. It is surprisingly found that the electrical conductivity for MWCNTs/PEH composites with high MWCNT concentrations increases obviously with annealing time of 40 min and the maximum increment approaches about 3 orders of magnitude with annealing time of 120 min. The increase of electrical conductivity of MWCNTs/PEH composites depends on MWCNT content, MWCNT aspect ratio and annealing time. SEM results clearly reveal that micrometer-sized MWCNT aggregates are broken down and more loosely packed MWCNT networks form due to annealing. Different types of networks in the composites are responsible for the evolutions of rheological (MWCNT network and PEH chain-MWCNT combined network) and electrical conductivity properties (tube−tube contacting MWCNT network). The reconstruction of MWCNT network during annealing is attributed to rotational diffusion of MWCNTs in PEH matrix at high temperature and the length of MWCNTs shows significant effect on this. The obvious enhancements of electrical conductivities can be ascribed to the thermal annealing-induced formation of loosely packed more homogeneous networks through non-Brownian motions.

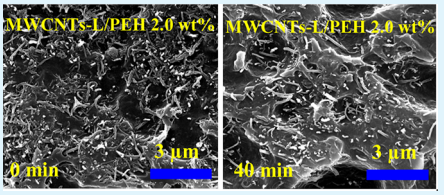

KEYWORDS: *polyethylene, carbon nanotube, aspect ratio, network, diffusion, electrical conductivity*

1. INTRODUCTION

Many applications of polymeric materials, such as electrodes, electrostatic dissipation, electromagnetic radiation shielding, and conductive adhesives, require electrical conductivity. Addition of electrically conductive fillers to polymers could effectively increase the electrical conductivity of polymers. Carbon nanotubes (CNTs) have attracted much attention since their discovery because of their fascinating physical properties and unique structures in various disciplines.[1,2] One of the most attractive applications is using CNTs as both strong reinforcing and electrically conductive fillers to prepare polymer composites. Indeed, the combination of high conductivity from CNTs with the flexibility and easy processability of polymers is highly desired. Composite materials with such unique properties are likely to facilitate new applications, such as lightweight radiation shields for use by NASA in outer space,[3−6] spatially and temporally controlled shape memory process for electrically conductive CNTs/polymer composites,[7] polymer based smart conductive materials as polymer sensors,[8] multifunctional freestanding CNTs/polymer thin films for energy conversion,[9] and so on. CNTs are proven to be one of the excellent fillers due to their low density, high aspect ratio, large specific surface area and high electrical conductivity for polymer composites to improve the electrical conductivity,[10] thermal conductivity[11] and mechanical properties.[12] It was demonstrated that the CNT network in polymer matrix would contribute to the prominent enhancements of physical properties of CNT/polymer composites due to modifications of heat and electrical current conductions or mechanical stress transfer.[13,14] Aspect ratio of CNTs is considered as the key factor to influence the CNT network formation and the corresponding percolation threshold of CNT/polymer composites. However, effective dispersion of CNTs with high aspect ratio in polymer matrix has proven difficult, which results in deteriorate properties compared with the expected electrical and mechanical properties of polymer composites in the case of ideal individual CNT dispersion.[15−17] Therefore, the interfacial interactions between CNTs and polymer matrix and the CNT network formation and reconstruction in polymer matrix play key roles to the final material properties.

Received: June 13, 2012
Accepted: November 22, 2012
Published: November 22, 2012

 © 2012 American Chemical Society dx.doi.org/10.1021/am302597f | *ACS Appl. Mater. Interfaces* 2012, 4, 6468−6478

The dispersion state of CNTs and reconstruction of CNT network in CNT/polymer composites are related to the blending methods and processing conditions.[18−20] Four main methods are commonly used to prepare CNT/polymer composites: solution blending,[21] in situ polymerization,[22] polymer grafting[23] and melt blending.[24] Melt blending is the most convenient method to prepare CNT-based polymer composites. However, lots of studies have shown that the melt blending can result in the loss of electrical conductivity and induce much lower electrical conductivity at a given CNT concentration.[25,26] By this method CNT network can be strongly affected by shear, which induces a breakage of CNT network, and then the method becomes less effective on dispersing CNTs in polymers especially at higher CNT loadings.[18,27] Comparatively, solution blending is much tender and more effective to obtain better dispersion of CNTs due to the low solution viscosity, and CNTs tend to randomly disperse as well.[28]

Recently several groups found that the electrical conductivity properties of CNT/polymer, carbon fibers/polymer, or carbon black/polymer composites prepared by melting blending could be improved by thermal annealing, which was explained by the filler particle reaggregation and the reconstruction of filler particle network in polymer matrices.[29−34] Cipriano et al. prepared MWCNTs/polystyrene and carbon nanofibers/polystyrene composites by melt blending and found that the electrical conductivities of the composites can be improved by thermal annealing at above the glass transition temperature of polystyrene, which was ascribed to the reestablished MWCNT networks due to annealing.[29] Annealing above the melting temperature for semicrystalline polymers or above the glass transition temperature for noncrystalline polymers can significantly improve the electrical conductivities, for examples, of the melt blended MWCNTs/polycarbonate composites[30] or MWCNTs/polyurethane composites,[31] because of the reformation of the conducting MWCNT networks described by a combination of MWCNT reaggregation and network formation. Pan et al. reported that annealing could cause electrical conductivity jump for MWCNTs/polypropylene composites, which was attributed to reaggregation of MWCNTs and the subsequent formation of the loosely packed MWCNT network during annealing.[32] Similar phenomenon was observed for carbon black (CB)-filled high density polyethylene composites.[33] Skipa et al. studied the shear-induced MWCNT network destruction and network building-up during annealing for the melt blended MWCNTs/polycarbonate composites by simultaneous time-resolved measurements of electrical conductivity and rheological properties.[34] All the above investigations demonstrate that the reaggregation of filler particles and reconstruction of filler particle networks could affect the material properties, including rheological, electrical conductivity, and thermal conductivity properties.

It is of great importance to investigate the CNT network formation and reconstruction of CNT aggregates into the loosely packed CNT network to gain insight into the mechanism for enhancements of electrical conductivity properties for CNT-filled polymer composites, especially for the more extensively applied composites using polyolefins as the matrix materials. Up to now, there have been few studies reporting the influences of CNT features, i.e. structural parameters, dispersion state, surface treatments, and interactions with polymer matrices, on the reconstruction of CNT networks in polyolefin composites due to thermal annealing. Moreover, the mechanism and the driving force for reconstruction of CNT network in the polymer matrices and on what extend it is related to the material properties have not been understood yet.

In this work, we take the aspect ratio (AR) of multiwalled carbon nanotubes (MWCNTs) as the key factor to study its influences on MWCNT network formation and reconstruction and the corresponding electrical conductivity properties for MWCNTs/statistical copolymer of ethylene and 1-hexene [poly(ethylene-*co*-hexene), PEH] composites prepared by solution blending method. The reasons for us to choose PEH as the polymer matrix are given as follows. The first reason is that the relevant studies in this field using polyolefin/MWCNT composites are sparsely reported. The second reason is that PEH as one type of short chain-branched linear polyethylene (with low branching density) is stable and not easily cross-linked or degraded at the temperatures used in this work. The thermally stable properties of PEH provide good background for the rheological and electrical conductivity measurements in the work. The third reason is that MWCNTs can be well-dispersed in PEH matrix with no need of any chemical modifications on the MWCNT surface. The good dispersion of MWCNTs in PEH matrix is prerequisite for any further studies. Two types of MWCNTs with different lengths (that is to say, with low and high aspect ratios) were chosen, respectively, as fillers to prepare MWCNTs/PEH composites. The evolutions of rheological and electrical conductivity properties with annealing time at the temperature higher than the melting point of PEH matrix for MWCNTs/PEH composites with different MWCNT concentrations were examined. The driving force for MWCNT reaggregation and the reconstruction of MWCNT network are proposed. Our study might contribute the basic understanding of CNT reaggregation and CNT network reconstruction in polymer matrix to the new polymer composite material development in general.

2. EXPERIMENTAL SECTION

2.1. Materials. Statistical copolymer of ethylene and 1-hexene, poly(ethylene-*co*-hexene) (PEH) (Exceed 1018CA) was synthesized with metallocene catalysts and supplied by ExxonMobil Co. Ltd. PEH had the weight average molecular mass, M_w, of 125 kg/mol, the number average molecular mass, M_n, of 79 kg/mol, and the polydispersity, M_w/M_n, of 1.6. Two types of multiwalled carbon nanotubes with low and high aspect ratios, respectively, were supplied by the ChengDu Organic Chemistry Co. Ltd., Chinese Academy of Sciences [MWCNTs-S, average diameters of more than 50 nm, average lengths of 0.5−2.0 μm, specific surface area (SSA) higher than 40 m^2/g, purity higher than 95%, ash content less than 1.5%; MWCNTs-L, average diameters of 10−20 nm, average length of about 30 μm, specific surface area (SSA) higher than 200 m^2/g, purity higher than 95%, and ash content less than 1.5%.] MWCNTs-S and MWCNTs-L were produced by the chemical vapor deposition (CVD) method. The other reagents, xylene and methanol, were purchased from the Beijing Chemical Reagents Company and used as received.

2.2. Preparation of MWCNTs/PEH Composites. An adapted hot coagulation was applied to prepare MWCNTs/PEH composites, similar to the method used by Haggenmueller et al.[35] Coagulation had been used commonly as an efficient method since it could provide better dispersion of carbon nanotubes in polymer matrix. PEH was first dissolved in xylene at PEH concentration of 30 mg/mL at 120 °C. MWCNTs were dispersed in xylene at MWCNT concentration of 0.25 wt % and the suspension was sonicated for 2 h to break up the MWCNT bundles. The MWCNTs/xylene suspension was transferred into an ultrasonic bath with temperature set at 100 °C and then the hot PEH/xylene solution was added into MWCNTs/xylene suspension. With further sonication for 10 min, the suspension was poured into a large amount of cold methanol. After filtration and

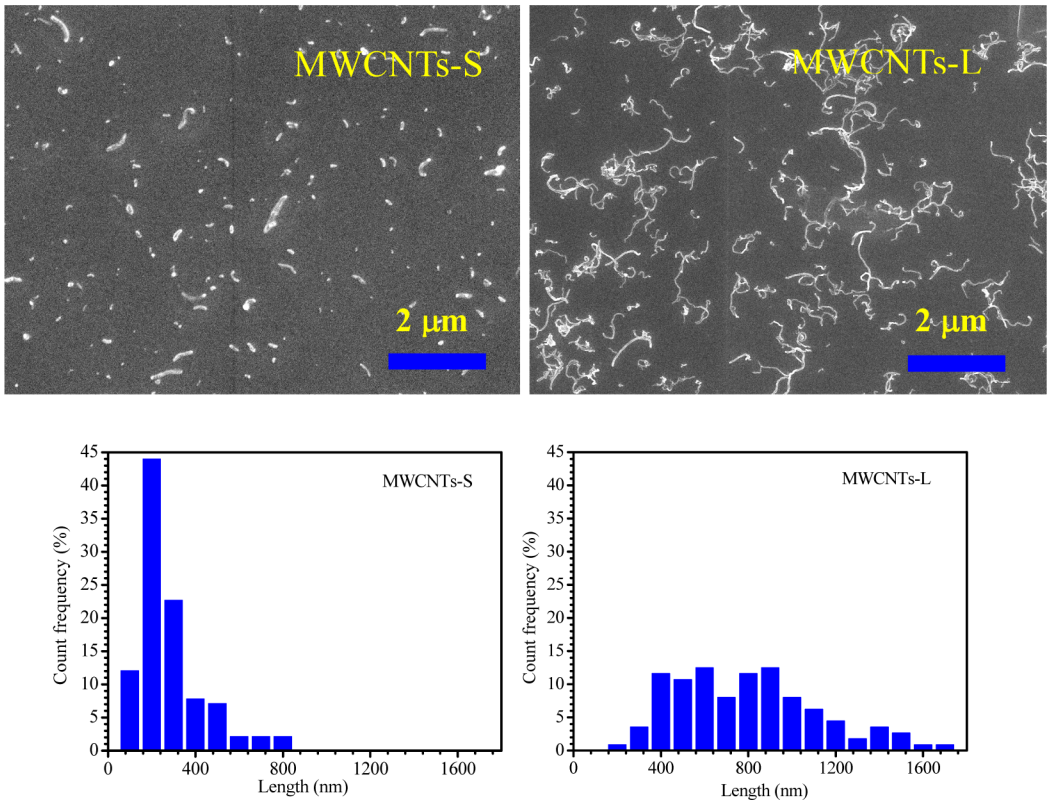

Figure 1. SEM micrographs and corresponding length distributions for MWCNTs-S and MWCNTs-L.

drying in vacuum at 70 °C for 48 h, MWCNTs/PEH composite was obtained. MWCNTs/PEH composites with different MWCNT concentrations ranging from 0.5 to 10.0 wt % were prepared. Note that MWCNTs here refer to both of MWCNTs-S and MWCNTs-L. Neat PEH was subjected to the same preparation procedure for comparison study purpose.

2.3. Annealing Process for MWCNTs/PEH Composites. The effects of annealing on the rheological, electrical conductivity properties and morphology of MWCNTs/PEH composites were measured, respectively. The composite samples for rheological frequency sweep measurements were annealed at 160 °C for 2 h without shear in a stress-controlled rheometer (TA-AR2000, TA Instruments, USA). The annealed samples for electrical conductivity measurements and SEM observations were prepared as follows. The composite samples were enclosed into an airproof aluminum box, which was put in an oil bath set at 160 °C for different time, and then was quenched into liquid nitrogen.

2.4. Scanning Electron Microscope (SEM). MWCNTs were ultrasonically dispersed in xylene for 2 h and a drop of the suspension diluted with ethanol was placed on aluminum foil. After the solvent was evaporated, MWCNTs on the aluminum foil were subjected to SEM (Hitachi S-530, Japan) observation to evaluate the lengths and diameters of MWCNTs by using the ImageJ Software (NIH, USA). Then, the average MWCNT aspect ratios (AR) could be estimated.

For SEM observation on bulk morphologies of MWCNTs/PEH composites, the composite samples were fractured in liquid nitrogen. Then the fractured surfaces of the samples were etched by 1 wt % solution of potassium permanganate in a mixture of sulfuric acid, orthophosphoric acid and water for an appropriate time.[36] The fractured samples were washed with a mixture of hydrogen peroxide and water (1/9), and then were dried in vacuum oven. The fractured surfaces of the composite samples were coated with gold before observation by using a field-emission SEM (INSPECT-F, FEI, Finland).

2.5. Optical Microscope (OM). The MWCNTs/PEH composites with 0.5 wt % MWCNT concentration were compressed into films with thickness of about 30 μm at 160 °C for OM observation. Optical microscope (Olympus BX 51, Japan) equipped with CCD camera (Daheng, Beijing, China) was used to examine the dispersion state of MWCNTs in PEH matrix at the micrometer scale.

2.6. Rheological Measurements. Rheological measurements on MWCNTs/PEH composites were performed on a stress-controlled rheometer (TA-AR2000, TA Instruments, USA) with 25 mm parallel plates under nitrogen blanket. Before rheological measurements, the dried MWCNTs/PEH composites were pressed at 160 °C in vacuum into disks with thickness of 1 mm and diameter of 25 mm using stainless steel dies. Strain sweeps were performed with the fixed frequency of 1 rad/s at 160 °C to determine the linear viscoelastic regime. According to the strain sweep curves, the linear viscoelastic regime for MWCNTs/PEH composites with higher MWCNT concentrations is within 1%. Therefore, to grantee linear response and sufficient toques of the rheometer, the strain of 1% was selected for all the followed rheological measurements. Oscillatory frequency sweeps ranging from 0.1 to 500 rad/s with the fixed strain of 1% were performed at 160 °C for MWCNTs/PEH composites. After the sample loading, an approximate 5 min equilibrium time was applied prior to each frequency sweep.

2.7. Electrical Conductivity Measurements. The MWCNTs/PEH composites were compressed in vacuum at 160 °C for 3 min to obtain samples with rectangular dimensions of length 10 mm x width 5 mm x thickness 1 mm. After thermal annealing treatments (described in section 2.3.) the samples were taken out for electrical conductivity measurements. Silver paste was coated on the left and right plane surfaces of the sample bar to ensure good contacts of the sample surfaces with electrodes of the electrometer. The resistance between two silver paste marks along the specimen length direction was measured at room temperature at a direct current voltage of 1 V with an automatic measurement system, for which the $I-V$ data were recorded by a computer. The electrical conductivity was calculated by the relation of $\sigma = L/RS$, where σ was the electrical conductivity, L was the length of the sample, R was the resistance and S was the cross section area of the sample. Electrical conductivity was estimated by a two-probe method on the Keithley 4200 semiconductor characterization system (Keithley 4200-SCS, Keithley Instruments Inc.,

Cleveland, OH, USA), which enabled high accuracy DC measurements of IV characteristics over a wide range (1.05 pA to 105 mA; 210 mV to 210 V). Three specimens for each composite were tested with three data points taken on each specimen.

3. RESULTS AND DISCUSSION

3.1. SEM Characterization of MWCNTs. The key factor in this study is the aspect ratio and length of MWCNTs, which could affect the MWCNT network formation and reconstruction as we will discuss in later sections. SEM micrographs were taken to estimate the aspect ratios of MWCNTs. Figure 1 shows typical SEM micrographs and the corresponding length distributions for MWCNTs-S and MWCNTs-L. The average lengths are 230 nm for MWCNTs-S and 750 nm for MWCNTs-L. The average diameters of 53 (± 11) nm for MWCNTs-S and 24 (± 4) nm for MWCNTs-L are obtained from the same SEM micrographs as shown in Figure 1. The above average diameter values of MWCNTs are consistent with the diameter values provided by the producer. Thus, the average aspect ratios (AR) for MWCNTs-S and MWCNTs-L can be estimated as 4 and 31, respectively.

3.2. MWCNT Dispersion in PEH Matrix. The disperse states of MWCNTs in PEH matrix at the micrometer scale could be observed by using optical microscopy (OM) and the typical results are shown in Figure 2. Note that to remove the

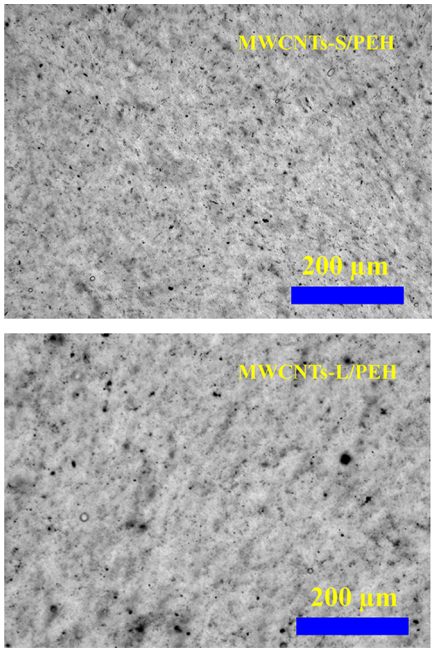

Figure 2. Optical micrographs for MWCNTs-S/PEH and MWCNTs-L/PEH composites with MWCNTs-S and MWCNTs-L concentration of 0.5 wt % in the molten state at 160 °C.

effect of crystalline morphology of PEH matrix, the MWCNTs/PEH composites were melted at 160 °C to keep PEH matrix in amorphous molten state between cover glasses for the OM observation. Further note that the equilibrium meting point of PEH is about 142 °C.[29] Because MWCNTs absorb light, the MWCNTs/PEH composites with MWCNT concentration of 0.5 wt % are suitable for OM observation. It can be seen from Figure 2 that both MWCNTs-S and MWCNTs-L are relatively uniformly dispersed in PEH matrix, respectively, except for small portions of black isolated MWCNT aggregates at the micrometer scale (the black fiber-like or dot-like MWCNT aggregates). In addition, dispersion of MWCNTs-S in PEH matrix looks more homogeneous than dispersion of MWCNTs-L in PEH matrix. Dispersion of MWCNTs in PEH matrix at higher resolution can be seen more clearly by using SEM measurements. Figure 3 shows SEM micrographs of etched

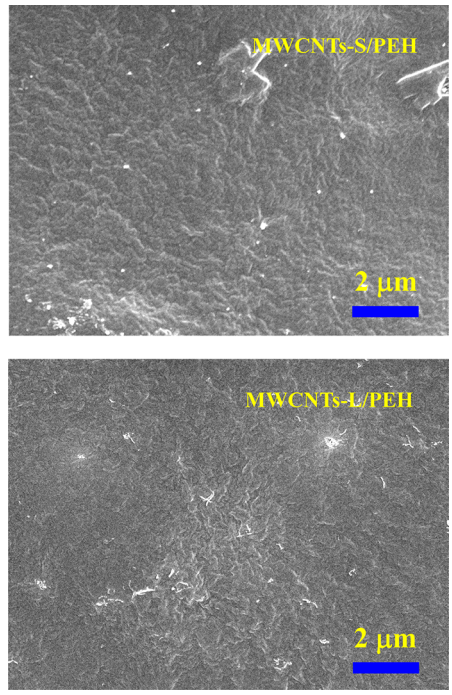

Figure 3. SEM micrographs of etched surfaces of MWCNTs-S/PEH and MWCNTs-L/PEH composites with 0.5 wt % MWCNTs-S and MWCNTs-L concentration, respectively.

surfaces of MWCNTs-S/PEH and MWCNTs-L/PEH composites with 0.5 wt % MWCNTs-S and MWCNTs-L concentration, respectively. It can be seen that the dispersion of MWCNTs in PEH matrix for the examined MWCNTs/PEH composites is overall homogeneous with only sparse isolated MWCNT aggregates. Because the fracture procedure for the composite samples separates the tubes into two fractured surfaces, and only the exposed MWCNTs on etched surfaces can be observed by SEM, the quantity of the observable MWCNTs on one surface might not represent the real MWCNT concentration in the composites. The length and diameter differences are also clearly seen for MWCNTs-L and MWCNTs-S, which are dispersed in PEH matrix. The relatively homogeneous dispersion of MWCNTs in PEH matrix for the solution blended MWCNTs/PEH composites is a prerequisite for our further studies. It is noted that MWCNTs can be better dispersed into polyethylene than polypropylene and this difference might be due to the linear chain structure of polyethylene. An even better dispersion of MWCNTs in PEH matrix can be obtained through the chemical modifications on MWCNT surfaces. However, the chemical modification process usually shortens the lengths of MWCNTs. Therefore, chemical modification was not considered in this work because the obtained MWCNT dispersions were satisfied for further studies.

3.3. Formation of MWCNT Network in PEH Matrix. In order to determine the linear viscoelastic regime for MWCNTs/PEH composites strain sweeps were carried out.

Figure 4 shows the changes of storage modulus, G', during strain sweeps at the fixed frequency of 1.0 rad/s and 160 °C for

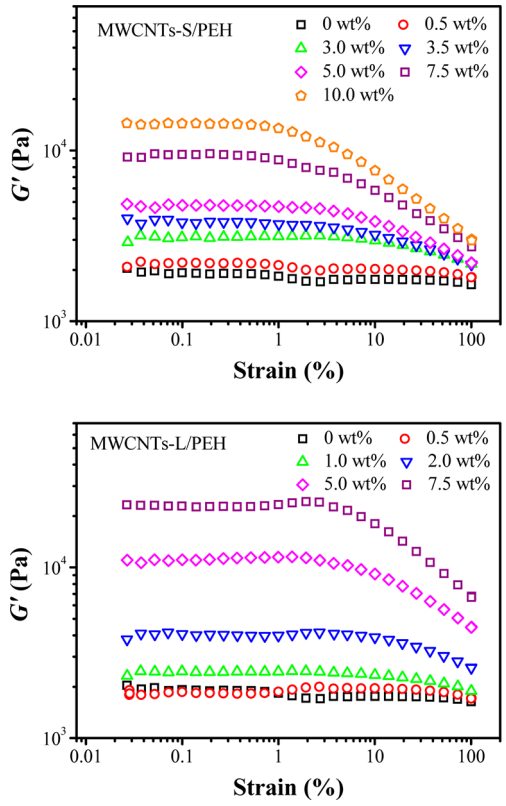

Figure 4. Changes of storage modulus, G', during strain sweeps at the fixed frequency of 1.0 rad/s and 160 °C for MWCNTs-S/PEH and MWCNTs-L/PEH composites with different MWCNT concentrations.

MWCNTs-S/PEH and MWCNTs-L/PEH composites with different MWCNT concentrations. Storage moduli, G', of MWCNTs/PEH composites at the low strains are largely enhanced by increasing the MWCNT concentration. More interesting is that the transitions from linear to nonlinear regimes shift to the lower shear strains with increasing MWCNT concentration at above the percolated MWCNT concentrations (values shown in Figure 5) when MWCNT network forms, which is attributed to the shear-induced orientation of MWCNT network.[37] To make sure linear response of MWCNTs/PEH composites and grantee sufficient torques for rheological measurements, oscillatory rheological measurements hereafter were conducted at the fixed strain of 1%. It can be further observed that MWCNTs-L is more efficient to increase storage modulus than MWCNTs-S at the same concentration for the composites because MWCNTs-L have higher aspect ratios than MWCNTs-S. This result is understandable from the geometry consideration because higher aspect ratio will make it easier for MWCNTs to contact with each other and form a continuous network path. As a consequence, the higher aspect ratio MWCNTs tend to give the lower percolation threshold for the composites, as will be indicated in details in Figure 5.[38,39] Furthermore, the critical strains of linear viscoelastic regime for MWCNTs-S/PEH and MWCNTs-L/PEH composites at 7.5 wt % concentration (above the percolation thresholds) are about 1 and 3%, respectively, because the entangled network structure of

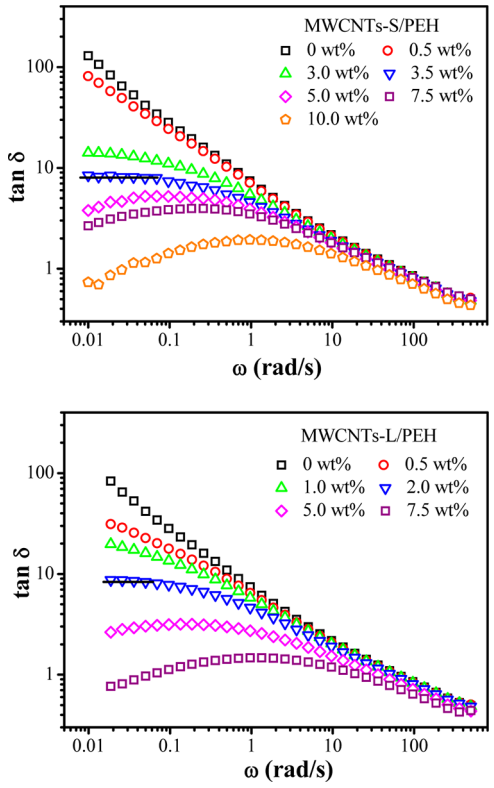

Figure 5. Frequency dependences of tan δ at the fixed strain of 1% (within the linear viscoelasticity regime) and 160 °C for MWCNTs-S/PEH and MWCNTs-L/PEH composites with different concentrations of MWCNTs-S and MWCNTs-L. The solid lines are drawn for the guide to eye.

MWCNTs-L has a higher potential to maintain the network intactness to applied shear deformation than that of MWCNTs-S, thus requesting a higher critical shear strain.[40,41]

Changes in the rheological parameter, tan δ, during the frequency sweeps provide confirmative fingerprints for indicating the MWCNT network formation. Figure 5 shows frequency dependences of tan δ at the fixed strain of 1% for the MWCNTs/PEH composites with different concentrations of MWCNTs-S and MWCNTs-L in the molten states at 160 °C. The frequency independence of tan δ reflects the solid-like elastic to liquid-like fluid transition, indicating a critical MWCNT concentration for MWCNT network formation in PEH matrix. Figure 5 clearly shows that tan δ decreases with increasing frequency at above the critical MWCNT concentration, indicating typical viscoelastic property, and tan δ becomes independent of frequency at low frequencies at the critical MWCNT concentration, which indicates the typical solid-like to liquid-like transition, usually found in the particle-filled polymer composites with polymer−particle interactions.[40,42,43] The critical MWCNT concentration (also called the percolation threshold) for MWCNTs-S/PEH composites is about 3.5 wt %. The percolation threshold for MWCNTs-L/PEH composites is about 2.0 wt %. The difference of percolation threshold values between MWCNTs-S/PEH and MWCNTs-L/PEH composites is ascribed to different MWCNT aspect ratios (AR), more specifically, a larger AR corresponding to a lower percolation threshold.[24,44−46] The percolation thresholds in this study are coincident with those for other MWCNTs/polymer composites prepared by solution

dx.doi.org/10.1021/am302597f | ACS Appl. Mater. Interfaces 2012, 4, 6468−6478

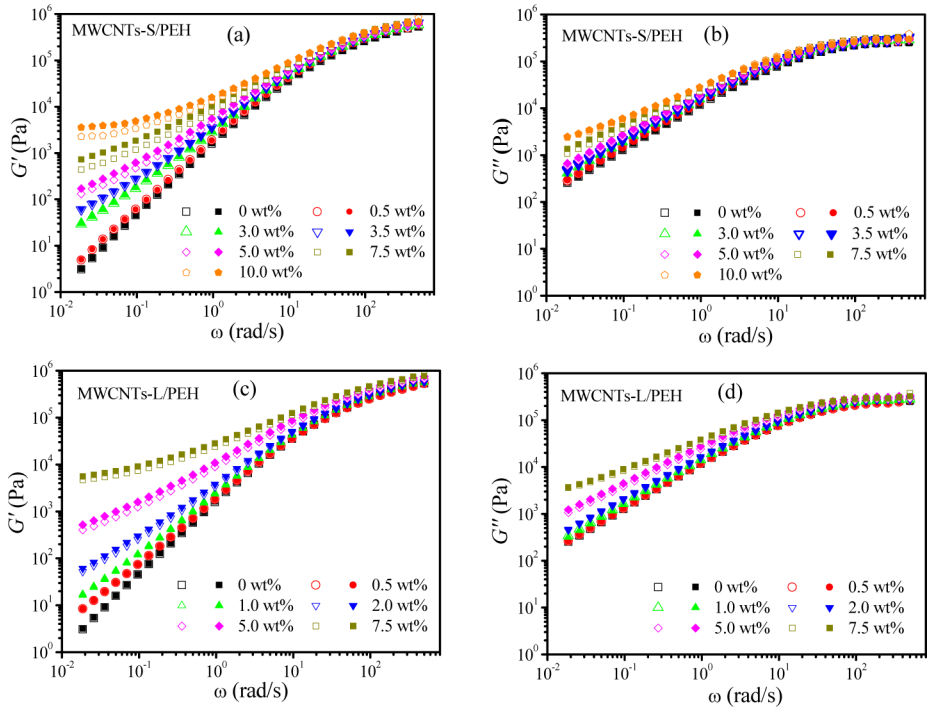

Figure 6. (a, c) Changes in storage modulus G' and (b, d) loss modulus G'' with frequency with the fixed strain of 1% at 160 °C for MWCNTs/PEH composites with different MWCNT concentrations without annealing (blank symbols) and with annealing at 160 °C for 2 h before frequency sweeps (solid symbols).

and melting blending processes in the literature considering the aspect ratio differences.[47−49]

3.4. Reconstruction of MWCNT Network Due to Annealing as Measured by Rheology. The effect of reconstruction of MWCNT network on the evolution of rheological properties for MWCNTs/PEH composites due to annealing was investigated by measuring frequency sweeps in molten states at 160 °C for the composite samples without annealing and with annealing at 160 °C for 2 h, respectively. The changes of storage modulus, G', and lose modulus, G'', with frequency with the fixed strain of 1% at 160 °C for MWCNTs/PEH composites without annealing and with annealing at 160 °C for 2 h before frequency sweeps are shown in Figure 6. Note that MWCNTs-L have higher aspect ratio than MWCNTs-S, therefore, at a given MWCNT concentration, MWCNTs-L/PEH composites have higher G' than MWCNTs-S/PEH composites as seen from Figures 6a and 6c. It is interesting to find that for both MWCNTs-S/PEH and MWCNTs-L/PEH composites, G' keeps almost unchanged between the two frequency sweeps of the composites without and with annealing when MWCNT concentrations are below the percolation thresholds; however, when MWCNT concentrations are above the percolation thresholds, G' becomes obviously higher for the composite samples with annealing, and the increase of G' becomes more prominent with increasing MWCNT concentration. This result indicates that the annealing-induced increase of G' is related to reconstruction of MWCNT network in PEH matrix, that is to say, to formation of more homogeneous MWCNT network, which is consistent with other reports that carbon fibers or carbon black aggregates can rearrange themselves to form more homogeneous networks during annealing.[33,50]

Figure 6 also shows that annealing has smaller effect on increase of G' at above the percolation thresholds for MWCNTs-L/PEH composites than for MWCNTs-S/PEH composites. This is because that during annealing the reconstruction of MWCNTs-L network is slower than that of MWCNTs-S network in PEH matrix and the more discussion about this difference will be provided in the later section.

Unlike G', the changes in loss modulus G'' due to annealing as shown in panels b and d in Figure 6 are subtle even when the MWCNT concentrations are above the percolation thresholds for both MWCNTs-S/PEH and MWCNTs-L/PEH composites. This is due to the elastic origin of MWCNT networks. Generally, the deformation of tube network is primarily reflected through the elastic properties of the composites, which is the reason why more remarkable changes due to the reconstruction of MWCNT network can be observed for G' than G''.[28,29]

To further confirm the reconstruction of MWCNT networks in PEH matrix, we measured the changes in storage modulus with time during annealing at 160 °C for MWCNTs/PEH composites with MWCNT concentrations above the percolation thresholds and the results are displayed in Figure 7. For both MWCNTs-S/PEH and MWCNTs-L/PEH composites, the changes of G' with annealing time can be separated by two stages. In the first stage, G' keeps slightly increasing with annealing time, while beyond a critical annealing time marked as t_p (also called the dynamic percolation time[50]), G' increases remarkably with further annealing time. From the viewpoint of colloids, such a separation can be explained by flocculation due to rearrangement and agglomeration of MWCNTs in PEH melts. After t_p, G' continuously increases over time, indicating a further development of reconstruction of MWCNT networks in the composites. According to the Einstein−Stokes Law,[51] the flocculation rate of filled particles is controlled by the polymer matrix viscosity and the sizes of filled particles (or aggregates). Thus, the key factors to affect t_p for the composites are the

dx.doi.org/10.1021/am302597f | ACS Appl. Mater. Interfaces 2012, 4, 6468−6478

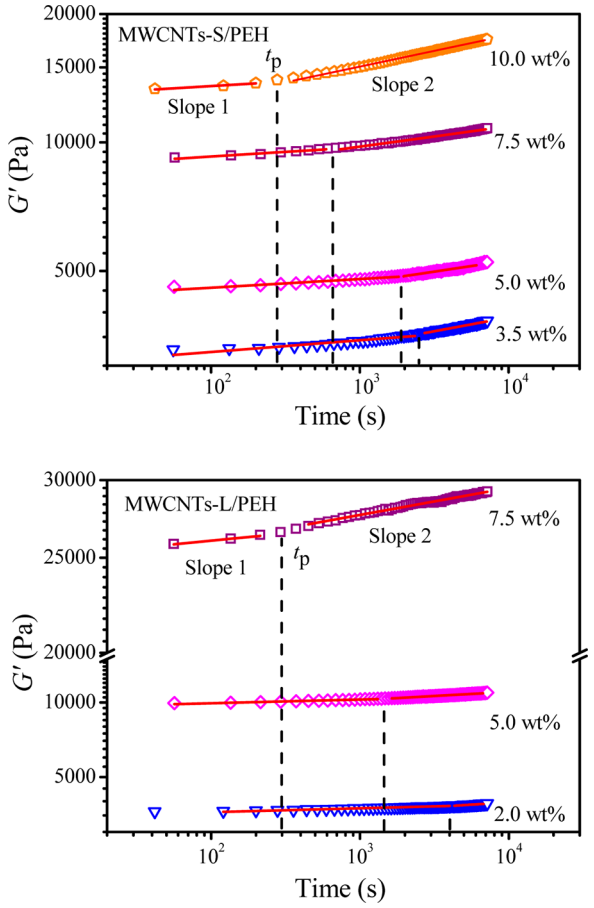

Figure 7. Changes in storage modulus G', with time during annealing at 160 °C for MWCNTs-S/PEH and MWCNTs-L/PEH composites with different MWCNT concentrations above the percolation thresholds. Strain of 1% and frequency of 1.0 rad/s were applied for rheological measurements.

viscosity of PEH matrix and the sizes of MWCNT aggregates. With increasing MWCNT concentration, the increase of G' at $t > t_p$ becomes more prominent and t_p also shifts to the short time. At the given temperature, the remarkable increase of G' with time at $t > t_p$ is considered to be related to the dynamic reconstruction process of MWCNT networks. Similar rheological behaviors have been observed in other carbon nanotube-filled or carbon black-filled polymers.[30,33,52] The above results provide further support to the thought of reconstruction of MWCNT networks in MWCNTs/PEH composites.

Table 1 lists the values of t_p and the slopes of the two stages from the changes of storage modulus, G', with time during annealing at 160 °C for MWCNTs-S/PEH and MWCNTs-L/PEH composites with MWCNT concentrations above the percolation thresholds. For both types of composites, t_p decreases significantly with increasing MWCNT concentration. It was reported that rearrangement of filler network could occur during annealing for carbon fibers or carbon black aggregates.[33,50] The probabilities of contacts among MWCNTs through diffusion increase with increasing MWCNT concentration, thus, MWCNTs in the higher concentration composites rearrange easier to reconstruct networks, which leads to the decrease of t_p. Slope 1 keeps almost constant at 0.02 and 0.015 for MWCNTs-S/PEH and MWCNTs-L/PEH composites, respectively, whereas slope 2 increases significantly compared with slope 1 for both the composites. In details,

Table 1. Values of Critical Time, t_p, and Slopes of the Two Stages from Changes of Storage Modulus, G', with Time during Annealing at 160 °C for MWCNTs/PEH Composites with MWCNT Concentrations above the Percolation Thresholds

MWCNTs-S or -L (wt %)	slope 1	slope 2	t_p (s)
	MWCNTs-S		
3.5	0.02	0.06	2600
5.0	0.02	0.05	1900
7.5	0.02	0.05	600
10.0	0.02	0.07	250
	MWCNTs-L		
2.0	0.016	0.04	4000
5.0	0.015	0.03	1500
7.5	0.015	0.03	300

values of slope 2 vary from 0.05 to 0.07 for MWCNTs-S/PEH composites and from 0.03 to 0.04 for MWCNTs-L/PEH composites, respectively. The lower values of slope 2 for MWCNTs-L/PEH composites are due to the slower reconstruction progress for MWCNTs-L network, consistent with the results shown in Figure 6.

3.5. Influence of Annealing on Evolution of Electrical Conductivity of MWCNTs/PEH Composites. CNTs possess excellent electrical conductivity; however, how the CNT dispersion and reconstruction of CNT network functions to the electrical conductivity plays the key role for CNT/polymer composites. Figure 8 shows the changes of electrical conductivity with annealing time for MWCNTs/PEH

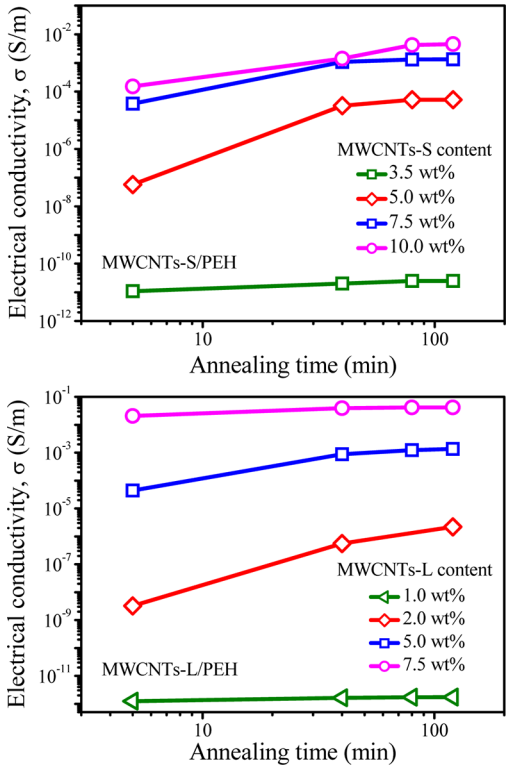

Figure 8. Evolutions of electrical conductivity, σ with annealing time for MWCNTs-S/PEH and MWCNTs-L/PEH composites with different MWCNT concentrations. The composite samples were annealed at 160 °C for different times and quenched into liquid nitrogen before measurements at room temperature.

dx.doi.org/10.1021/am302597f | ACS Appl. Mater. Interfaces 2012, 4, 6468−6478

composites. As can be seen from Figure 8, electrical conductivity increases to higher values and the gap for the composites with adjacent MWCNT concentrations becomes narrower with increasing MWCNT concentration because of increasing MWCNT network density. It is more interesting to find that electrical conductivity increases dramatically due to annealing. For examples, for 5.0 wt % MWCNTs-S/PEH composite, the electrical conductivity increases by 3 orders of magnitude to 5.6×10^{-5} S/m by annealing of 120 min, for 7.5 wt % MWCNTs-S/PEH composite, the electrical conductivity increases by less than 2 orders of magnitude to 1.28×10^{-3} S/m by annealing of 120 min, and for 10.0 wt % MWCNTs-S/PEH composite, the electrical conductivity increases by less than 2 orders of magnitude to 4.55×10^{-3} S/m by annealing of the same time; for 2.0 wt % MWCNTs-L/PEH composite, the electrical conductivity increases by less than 3 orders of magnitude to 2.2×10^{-6} S/m by annealing of 120 min, for 5.0 wt % MWCNTs-L/PEH composite, the electrical conductivity increases by less than 2 orders of magnitude to 1.35×10^{-6} S/m by annealing of 120 min, and for 7.5 wt % MWCNTs-L/PEH composite, the electrical conductivity increases by less than 1 order of magnitude to 4.17×10^{-2} S/m by annealing of the same time. Because of the significantly higher aspect ratio of 31 for MWCNTs-L than that of 4 for MWCNTs-S, MWCNTs-L can more easily form MWCNT networks with tube−tube contacts for the electron tunneling mechanism than MWCNTs-S can form, thus, the electrical conductivity of MWCNTs-L/PEH composites is much higher than that of MWCNTs-S/PEH composites at the same MWCNT concentration.[22,53−55] The above electron tunneling mechanism also explains that for MWCNTs-S/PEH composites the rheological percolation threshold concentration of 3.5 wt % (shown in Figure 5) is not sufficient to approach the electrical conductivity percolation threshold concentration as shown in Figure 8, in which 3.5 wt % MWCNTs-S/PEH composite shows slight increase of electrical conductivity with annealing time due to insufficient MWCNTs-S concentration in the composite for reconstruction of tube−tube contacted MWCNT network. The 1.0 wt % MWCNTs-L/PEH composite is the same case. However, at the given sufficient MWCNT concentrations, the increase of electrical conductivity for MWCNTs-S/PEH composites is much more prominent than that of MWCNTs-L/PEH composites apparently due to the slower reconstruction progress for MWCNTs-L network, such as for 7.5 wt % MWCNTs-S/PEH composite, the electrical conductivity increases by less than 2 orders of magnitude to 1.28×10^{-3} S/m after annealing of 120 min, whereas, for 7.5 wt % MWCNTs-L/PEH composite, the electrical conductivity increases by only less than 1 order of magnitude to 4.17×10^{-2} S/m after annealing of the same time.

It is worthwhile to emphasize that the evolution of rheological properties is not consistent with that of electrical conductivity property with annealing time for MWCNTs/PEH composites with different MWCNT concentrations. The results shown in Figures 6 and 7 indicate that at the low frequencies storage modulus, G', of MWCNTs/PEH composites with high MWCNT concentrations improves more significantly than that with low MWCNT concentrations during annealing. However, the results shown in Figure 8 indicate that electrical conductivity of MWCNTs/PEH composites with low MWCNT concentrations increases more significantly than that with high MWCNT concentrations during annealing. The different variation trends of storage modulus and electrical conductivity can be interpreted from the different mechanisms responsible for the rheological and electrical conductivity properties, respectively. The electrical conductivity property is dominated by the tube−tube contacted MWCNT network.[46] Annealing can induce MWCNT reaggregation and reconstruct MWCNT network with more homogeneous tube−tube contacts, thus leading to the increased electrical conductivity; the reconstruction process of MWCNT network results in an effective electrical conductivity increase when MWCNT concentration is sufficient high (5.0 wt % for MWCNTs-S/PEH composites and 2.0 wt % for MWCNTs-L/PEH composites as shown in Figure 8), and the electrical conductivity increase should become less prominent with further increasing MWCNT concentration because the initially formed MWCNT network at higher MWCNT concentration can have had sufficient tube−tube contacts and the effect from the reconstruction process of MWCNT network becomes less effective for further electrical conductivity increase (shown in Figure 8). However, the rheological properties at the low frequencies are dominated by two types of networks in the composites, MWCNT network and MWCNT-polymer chain network.[30,33,56] The reconstruction process of MWCNT network due to annealing enhances the homogeneity of MWCNT network and more polymer chains are entrapped or involved in MWCNT networks or into the newly formed MWCNT aggregates, which causes the storage modulus increase at the low frequencies; when MWCNT concentration increases the combination of MWCNTs and polymer chains becomes more significant with annealing time, thus the increase of storage modulus at the low frequencies becomes more obvious as shown in Figures 6 and 7. The tube−tube contacted MWCNT network for forming an electrical conductivity path should be more difficult to form than MWCNT-polymer chain combined network required to impede polymer chain mobility for rheological properties, leading to the higher MWCNT concentration required to approach the electrical conductivity percolation threshold, and the difference is more obvious when MWCNTs-S with low aspect ratio are added as the fillers. The difference between rheological and electrical conductivity percolation thresholds has been observed in lots of studies on CNT/polymer composites.[20,21,36,37,45] In spite of the fact that different types of networks are responsible for the observed different evolutions of rheological and electrical conductivity properties, the morphology of MWCNTs/PEH composites should change by an exclusive way when subjected to annealing, which provides more evidence to support the reconstruction process of MWCNT networks in PEH matrix as will be shown in the next section.

3.6. Influence of Annealing on Morphologies of MWCNTs/PEH Composites. To clearly show the annealing-induced morphological changes for MWCNTs/PEH composites, we performed SEM measurements. Figure 9 shows the typical SEM micrographs taken from etched fractured surfaces of MWCNTs-S/PEH composite with 3.5 wt % MWCNT concentration and MWCNTs-L/PEH composite with 2.0 wt % MWCNT concentration without annealing and with annealing for 40 min, respectively. The results demonstrate that MWCNT networks with dense MWCNT aggregates of micrometer sizes dominate the etched surfaces of the composites before annealing (micrographs at the left panel), which are induced by van der Waals attractions among MWCNTs, whereas the more loosely packed homogeneous MWCNT networks can be seen from the etched surfaces of the

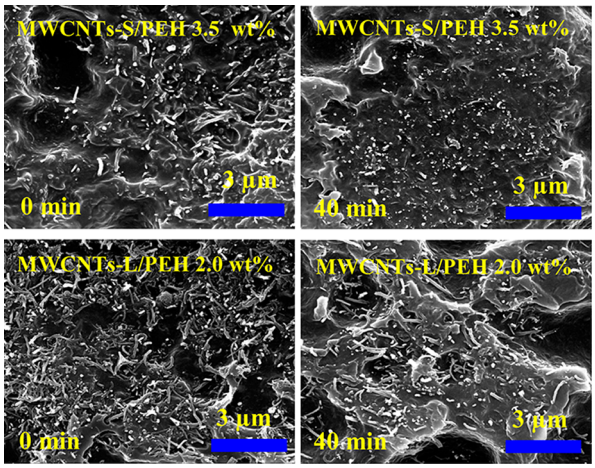

Figure 9. SEM micrographs taken from the etched fractured surfaces of MWCNTs-S/PEH composite with 3.5 wt % MWCNT concentration and MWCNTs-L/PEH composite with 2.0 wt % MWCNT concentration without annealing (0 min, left panel) and with annealing (40 min, right panel).

composites after thermal annealing for 40 min (micrographs at the right panel). Therefore, the thermal annealing process brings out the redistribution of the relatively large MWCNT aggregates and reformation of the more loosely packed MWCNT networks, which is considered as the key process to affect the evolutions of rheological and electrical conductivity properties for MWCNTs/PEH composites.

In the previous studies,[50,52,57,58] it was demonstrated that the dispersion of filler particles in polymer matrix was not in a thermodynamic equilibrium state. For the MWCNTs/PEH composites in this study, it is very likely that the structures in the composites prepared by the coagulation method are not thermodynamically stable.[59,60] The thermodynamically unstable MWCNT aggregates would most likely undergo gelation and network formation rather than macroscopic phase separation.[61,62] The attractive MWCNT−MWCNT interactions among the different MWCNT aggregation domains might be the driving force for the structural evolution and network reconstruction. Although the translational and/or rotational diffusions of the MWCNT aggregates of micrometer sizes may be limited, the MWCNTs are still able to reorient, even under non-Brownian conditions,[40,63,64] because the viscoelastic nature of polymer matrix. That is to say, the relaxation of polymer chains at the high annealing temperatures could facilitate the rearrangement of the dispersed MWCNTs. During the annealing procedure the relaxation of polymer chains in the MWCNT aggregation domains could help disassemble the MWCNT aggregates, which could also assist the formation of more loosely homogeneous MWCNT networks. The reconstruction of MWCNT network for MWCNTs/PEH composites during annealing is related to the rotational diffusion of MWCNTs because of the non-Brownian motion in PEH matrix at the temperature above the melting temperature of PEH. MWCNTs can be considered as long fibers in semidilute suspensions. The diffusion coefficient D of MWCNTs is provided by eq 1 as follows[62]

$$D = \frac{k_B T}{\zeta} \tag{1}$$

where k_B is the Boltzmann constant, and ζ is the friction constant of the long fibers; its inverse is called the mobility, which is expressed by eq 2 as follows:[62]

$$\zeta = \frac{\pi \eta_s L^3}{3\ln(\pi/\phi)} \tag{2}$$

where η_s is the viscosity of polymer matrix, ϕ is the volume fraction of fibers, and L is the fiber length. In this study, the average lengths of the tubes are 230 and 750 nm for MWCNTs-S and MWCNTs-L, respectively. Consequently, the diffusion coefficient of MWCNTs-S could be 35 times of that of MWCNTs-L. As a result, it is reasonably considered that due to the enhanced non-Brownian motion the reconstruction of MWCNT network by MWCNTs-S occurs more prominently than by MWCNTs-L for the composites at the same MWCNT volume concentration.

Note that for MWCNTs/PEH composites at MWCNT concentrations below the percolation thresholds, the increase in storage modulus due to annealing can be hardly found. This can be explained by large distances among MWCNTs at the low MWCNT concentrations. It is obvious that at the low MWCNT concentrations there is not a percolated MWCNT network formed in the composites and the distances for MWCNTs to diffuse to contact with each other are too far to reach. Some isolated MWCNT aggregates form, which puts on more difficulty for forming MWCNT network in PEH matrix, providing none of the electrical conductivity path spanning through the composites for appreciable electrical conductivity changes as well. Therefore, no increases for storage modulus and electrical conductivity with annealing time are observed for MWCNTs/PEH composites with low MWCNT concentrations particularly below the percolation thresholds.

4. CONCLUSIONS

In this work, multiwalled carbon nanotube-filled poly(ethylene-*co*-hexene) (MWCNTs/PEH) composites were prepared by solution blending. The evolutions of rheological and electrical conductivity properties with annealing time for MWCNTs/PEH composites were investigated mainly by rheological and electrical conductivity measurements, with particular attention given to the reconstruction of MWCNT network because of annealing. Two types of MWCNTs with low and high aspect ratios (4 and 31) were added, respectively as fillers into PEH matrix for comparison study purpose. It is found that annealing of MWCNTs/PEH composites at above the melting temperature of PEH matrix leads to increase of storage modulus at low frequencies and obvious enhancements of electrical conductivity. However, these kinds of changes can only be seen for MWCNTs/PEH composites with MWCNT concentrations above the percolation thresholds, which indicate that the reconstruction of MWCNT networks during annealing is crucial. More obvious changes of rheological and electrical conductivity properties during annealing are found for MWCNTs-S/PEH composites than for MWCNTs-L/PEH composites because MWCNTs-S have much higher diffusion coefficient than MWCNTs-L for the reconstruction process of MWCNT networks. The MWCNT−MWCNT interactions are considered to be the driving force for the reconstruction of MWCNT networks, which is accomplished through the relaxation of polymer chains and the non-Brownian motion of MWCNTs at the high thermal annealing temperature. SEM observation clearly reveals the formation of more loosely

packed homogeneous MWCNT networks in MWCNTs/PEH composites due to annealing, which contributes to the obviously enhanced electrical conductivity properties.

AUTHOR INFORMATION

Corresponding Author

*Tel.: +86 0551-3607703. Fax: +86 0551-3607703. E-mails: zgwang2@ustc.edu.cn (Z.G.W.); yhniu@iccas.ac.cn (Y.H.N.).

Notes

The authors declare no competing financial interest.

ACKNOWLEDGMENTS

Z.G.W. acknowledges the financial support from the National Science Foundation of China (51073145) and National Basic Research Program of China (2012CB025901). Y.H.N. acknowledges the financial support from the National Science Foundation of China (50803073). The project is also supported by the Open Research Fund of State Key Laboratory of Polymer Physics and Chemistry, Changchun Institute of Applied Chemistry, Chinese Academy of Sciences.

REFERENCES

(1) Iijima, S. *Nature* **1991**, *354*, 56−58.
(2) Iijima, S.; Ichihashi, T. *Nature* **1993**, *363*, 603−605.
(3) Dalton, A. B.; Collins, S.; Munoz, E.; Razal, J. M.; Ebron, V. H.; Ferraris, J. P.; Coleman, J. N.; Kim, B. G.; Baughman, R. H. *Nature* **2003**, *423*, 703−703.
(4) Ramasubramaniam, R.; Chen, J.; Liu, H. Y. *Appl. Phys. Lett.* **2003**, *83*, 2928−2930.
(5) Smith, J. G.; Connell, J. W.; Delozier, D. M.; Lillehei, P. T.; Watson, K. A.; Lin, Y.; Zhou, B.; Sun, Y. P. *Polymer* **2004**, *45*, 825−836.
(6) Yuan, W.; Che, J. F.; Chan-Park, M. B. *Chem. Mater.* **2011**, *23*, 4149−4157.
(7) Fei, G. X.; Li, G.; Wu, L. S.; Xia, H. S. *Soft Matter* **2012**, *8*, 5123−5126.
(8) Ferrreira, A.; Rocha, J. G.; Ansón-Casaos, A.; Martínez, M. T.; Vaz, F.; Lanceros-Mendez, S. *Sens. Actuators, A* **2012**, *178*, 10−16.
(9) Li, X. K.; Gittleson, F.; Carmo, M.; Sekol, R. C.; Taylor, A. D. *ACS Nano* **2012**, *6*, 1347−1356.
(10) Chang, C. M.; Liu, Y. L. *ACS Appl. Mater. Interfaces* **2011**, *3*, 2204−2208.
(11) Bonnet, P.; Sireude, D.; Garnier, B.; Chauvet, O. *Appl. Phys. Lett.* **2007**, *91*, 201910.
(12) Yu, M. F.; Files, B. S.; Arepalli, S.; Ruoff, R. S. *Phys. Rev. Lett.* **2000**, *84*, 5552−5555.
(13) Jancar, J.; Douglas, J. F.; Starr, F. W.; Kumar, S. K.; Cassagnau, P.; Lesser, A. J.; Sternstein, S. S.; Buehler, M. J. *Polymer* **2010**, *51*, 3321−3343.
(14) Andrews, R.; Weisenberger, M. *Curr. Opin. Solid State Mater. Sci.* **2004**, *8*, 31−37.
(15) Jin, Z.; Pramoda, K. P.; Xu, G.; Goh, S. H. *Chem. Phys. Lett.* **2001**, *337*, 43−47.
(16) Thostenson, E. T.; Ren, Z.; Chou, T. W. *Compos. Sci. Technol.* **2001**, *61*, 1899−1912.
(17) Sandler, J.; Shaffer, M. S. P.; Prasse, T.; Bauhofer, W.; Schulte, K.; Windle, A. H. *Polymer* **1999**, *40*, 5967−5971.
(18) Wu, D. F.; Wu, L.; Zhang, M. *J. Polym. Sci., Part B: Polym. Phys.* **2007**, *45*, 2239−2251.
(19) Ratna, D.; Abraham, T. N.; Siengchin, S.; Karger-Kocsis, J. *J. Polym. Sci., Part B: Polym. Phys.* **2009**, *47*, 1156−1165.
(20) Zhang, K.; Lim, J. Y.; Choi, H. J. *Diamond Relat. Mater.* **2009**, *18*, 316−318.
(21) Sabba, Y.; Thomas, E. L. *Macromolecules* **2004**, *37*, 4815−4820.
(22) Park, C.; Ounaies, Z.; Watson, K. A.; Crooks, R. E.; Smith, J.; Lowther, S. E.; Connell, J. W.; Siochi, E. J.; Harrison, J. S.; Clair, T. L. S. *Chem. Phys. Lett.* **2002**, *364*, 303−308.
(23) Fragneaud, B.; Masenelli-Varlot, K.; González-Montiel, A.; Terrones, M.; Cavaillé, J. Y. *Chem. Phys. Lett.* **2007**, *444*, 1−8.
(24) Pötschke, P.; Fornes, T. D.; Paul, D. R. *Polymer* **2002**, *43*, 3247−3255.
(25) Pötschke, P.; Dudkin, S. M.; Alig, I. *Polymer* **2003**, *44*, 5023−5030.
(26) Moniruzzaman, M.; Winey, K. I. *Macromolecules* **2006**, *39*, 5194−5205.
(27) Abbasi, S.; Carreau, P. J.; Derdouri, A. *Polymer* **2010**, *51*, 922−935.
(28) McNally, T.; Potschke, P.; Halley, P.; Murphy, M.; Martin, D.; Bell, S. E. J.; Brennan, G. P.; Bein, D.; Lemoine, P.; Quinn, J. P. *Polymer* **2005**, *46*, 8222−8232.
(29) Cipriano, B. H.; Kota, A. K.; Gershon, A. L.; Laskowski, C. J.; Kashiwagi, T.; Bruck, H. A.; Raghavan, S. R. *Polymer* **2008**, *49*, 4846−4851.
(30) Alig, I.; Skipa, T.; Lellinger, D.; Pötschke, P. *Polymer* **2008**, *49*, 3524−3532.
(31) Zhang, R.; Dowden, A.; Deng, H.; Baxendale, M.; Peijs, T. *Compos. Sci. Technol.* **2009**, *69*, 1499−1504.
(32) Pan, Y.; Cheng, H. K. F.; Li, L.; Chan, S. H.; Zhao, J.; Juay, Y. K. *J. Polym. Sci., Part B: Polym. Phys.* **2010**, *48*, 2238−2247.
(33) Cao, Q.; Song, Y.; Tan, Y.; Zheng, Q. *Polymer* **2009**, *50*, 6350−6356.
(34) Skipa, T.; Lellinger, D.; Böhm, W.; Saphiannikova, M.; Alig, I. *Polymer* **2010**, *51*, 201−210.
(35) Haggenmueller, R.; Fischer, J. E.; Winey, K. I. *Macromolecules* **2006**, *39*, 2964−2971.
(36) Yang, L.; Niu, Y. H.; Wang, H.; Wang, Z. G. *Polymer* **2009**, *50*, 2990−2998.
(37) Bokobza, L. *Polymer* **2007**, *48*, 4907−4920.
(38) Xu, Z. H.; Niu, Y. H.; Wang, Z. G.; Li, H.; Yang, L.; Qiu, J.; Wang, H. *ACS Appl. Mater. Interfaces* **2011**, *3*, 3744−3753.
(39) Huang, C. L.; Wang, C. *Carbon* **2011**, *49*, 2334−2344.
(40) Kharchenko, S. B.; Douglas, J. F.; Obrzut, J.; Grulke, E. A.; Migler, K. B. *Nat. Mater.* **2004**, *3*, 564−568.
(41) Xu, D. H.; Wang, Z. G.; Douglas, J. F. *Macromolecules* **2008**, *41*, 815−825.
(42) Xu, X. M.; Tao, X. L.; Zheng, Q. *Chin. J. Polym. Sci.* **2008**, *26*, 145−152.
(43) Agarwal, S.; Salovey, R. *Polym. Eng. Sci.* **1995**, *35*, 1241−1251.
(44) Li, J.; Ma, P. C.; Chow, W. S.; To, C. K.; Tang, B. Z.; Kim, J. K. *Adv. Funct. Mater.* **2007**, *17*, 3207−3215.
(45) Barrau, S.; Demont, P.; Perez, E.; Peigney, A.; Laurent, C.; Lacabanne, C. *Macromolecules* **2003**, *36*, 9678−9680.
(46) Du, F.; Scogna, R. C.; Zhou, W.; Brand, S.; Fischer, J. E.; Winey, K. I. *Macromolecules* **2004**, *37*, 9048−9055.
(47) Lee, S. H.; Cho, E.; Jeon, S. H.; Youn, J. R. *Carbon* **2007**, *45*, 2810−2822.
(48) McNally, T.; Pötschke, P.; Halley, P.; Murphy, M.; Martin, D.; Bell, S. E. J.; Brennan, G. P.; Bein, D.; Lemoine, P.; Quinn, J. P. *Polymer* **2005**, *46*, 8222−8232.
(49) Xu, Z. H.; Niu, Y. H.; Yang, L.; Xie, W. Y.; Li, H.; Gan, Z. H.; Wang, Z. G. *Polymer* **2010**, *51*, 730−737.
(50) Zhang, C.; Wang, P.; Ma, C. A.; Wu, G. Z.; Sumita, M. *Polymer* **2006**, *47*, 466−473.
(51) Allen, P. E. M.; Patrick, C. R. *Kinetics and Mechanisms of Polymerization Reactions−Applications of Physico-chemical Principles*; Wiley: New York, 1974.
(52) Cao, Q.; Song, Y.; Tan, Y.; Zheng, Q. *Carbon* **2010**, *48*, 4268−4275.
(53) Jiang, M. J.; Dang, Z. M.; Xu, H. P.; Yao, S. H.; Bai, J. *Appl. Phys. Lett.* **2007**, *91*, 072907.
(54) Yao, S. H.; Dang, Z. M.; Jiang, M. J.; Xu, H. P.; Bai, J. *Appl. Phys. Lett.* **2007**, *91*, 212901.

(55) Dang, Z. M.; Yuan, J. K.; Zha, J. W.; Zhou, T.; Li, S. T.; Hu, G. H. *Prog. Mater. Sci.* **2012**, *57*, 660−723.
(56) Pötschke, P.; Abdel-Goad, M.; Alig, I.; Dudkin, S.; Lellinger, D. *Polymer* **2004**, *45*, 8863−8870.
(57) Wong, M.; Paramsothy, M.; Xu, X. J.; Ren, Y.; Li, S.; Liao, K. *Polymer* **2003**, *44*, 7757−7764.
(58) Wessling, B. *Adv. Mater.* **1993**, *5*, 300−305.
(59) Ginzburg, V. V.; Balazs, A. C. *Macromolecules* **1999**, *32*, 5681−5688.
(60) Balazs, A. C.; Singh, C.; Zhulina, E. *Macromolecules* **1998**, *31*, 8370−8381.
(61) Russel, W. B.; Saville, D. A.; Schowalter, W. R. *Colloidal Dispersions*; Cambridge University Press: Cambridge, U.K., 1989; pp 488−503.
(62) Larson, R. G. *The Structure and Rheology of Complex Fluids*; Oxford University Press: New York, 1999; pp 291−297; pp 334−337.
(63) Ren, J. X.; Casanueva, B. F.; Mitchell, C. A.; Krishnamoorti, R. *Macromolecules* **2003**, *36*, 4188−4194.
(64) Solomon, M. J.; Almusallam, A. S.; Seefeldt, K. F.; Somwangthanaroj, A.; Varadan, P. *Macromolecules* **2001**, *34*, 1864−1872.